EasyChair Preprint

№ 15351

Subspace Methods for Dynamic Systems Identification with MOESP

Maria Fernanda Silva, Rodrigo Silva, Glauber Leite,
Thiago Cordeiro and Ícaro Araújo

November 1, 2024

Subspace Methods for Dynamic Systems Identification with MOESP

Maria Fernanda H. M. da Silva * **Rodrigo S. da Silva** *
Glauber R. Leite * **Thiago D. Cordeiro** * **Ícaro B. Q. de Araújo** *

* *Computing Institute, Federal University of Alagoas, Maceió, AL, Brazil, {mfhms, rss3, glauber, thiago, icaro} @ic.ufal.br*

Abstract: System identification is a pivotal field within control engineering, providing a strategic approach to control challenges when direct modeling of systems proves unfeasible. Using input and output data from the system under analysis, it becomes feasible to construct a mathematical model that captures its dynamics without fully understanding its internal mechanics. Among the various identification methods, the Multivariable Output Error State Space (MOESP) algorithm is distinguished by its straightforwardness, importance, and determinism, enabling the identification of systems represented by state equations. This study explores the steps of this algorithm and its application and validation in dynamic systems. Furthermore, the influence of estimated order, a free algorithm variable, is investigated through graphical and mathematical analysis. We used two examples of dynamic MIMO systems to validate the identification strategy explored in this work. A numerical simulation of a linear system represented the first system. The other constitutes a real nonlinear system. The results presented model evaluation metrics that show the efficacy of the methodology under study.

Keywords: System Identification, MOESP, Subspace Methods, State Space, Dynamic Systems.

1. INTRODUCTION

Creating mathematical models of a system's dynamics plays a vital role in performance optimization, predicting future behaviors of the system, and designing control techniques efficiently. Hence, system identification is essential because one can derive the models directly from experimental data. These systems reflect complexities that cut across large forbearing domains: industrial processes, biological frameworks, and environmental interactions, as discussed in Zhou et al. (2023).

Through these models, the internal dynamics of a system may be understood, along with the design and implementation of controllers that will realize optimal functionality. However, since many systems are highly complex and nonlinear, system identification is often challenging and requires robust methodologies and techniques to extract useful information from the available data.

The state-space approach stands out among other system representations due to its better adaptation to nonlinearity problems and simple, flexible, and matrix-based representation. This characteristic allows for the use of algebraic frameworks in the process of system identification.

In this context, the Multivariable Output Error State-Space (MOESP) algorithm is particularly notable as a system identification methodology for its efficacy in representing systems via state-space equations De Moor et al. (1997). This algorithm provides a robust and efficient parameter estimation methodology that facilitates precise characterization of the system's dynamics. Consequently, by delving into and understanding the mechanics of the MOESP algorithm, it becomes feasible to broaden the range of systems that can be effectively modeled and controlled.

As discussed in Bauer (2001), selecting the correct system order is critical in system identification. An overly high system order can lead to overfitting, where the model becomes too complex and captures noise rather than the underlying system dynamics—on the other hand, selecting a system order that is too low results in underfitting, where the model fails to capture essential dynamics, leading to inaccurate predictions. Therefore, balancing model complexity and accuracy is vital, and information criteria such as AIC and BIC are commonly utilized to guide the selection of an appropriate system order.

In this study, we explore the steps of this MOESP algorithm and the influence of estimated order through graphical and mathematical analysis. Two examples of dynamic MIMO systems were used to validate the identification strategy explored in this work. We used a numerical simulation of a linear system as the first system, and the second one constitutes a real nonlinear system. The results presented model evaluation metrics that show the efficacy of the methodology under study.

The structure of this paper is as follows. Section 2 explores the theories used in applying MOESP to the data. Section 3 details the algorithm's operation and assimilates the theory presented into practice. Section 4 corresponds to the results of MOESP in two dynamic systems (simulated and real coupled tank systems). Finally, the conclusion section provides general considerations about the work and discusses possible future works.

2. MATERIALS AND METHODS

2.1 Subspace Identification

In engineering, simple mathematical models can clarify the dynamics of a system and facilitate the control process. The branch of engineering known as system modeling and identification explores methodologies to address the challenges of deducing a system's mathematical model. Experts classify situations that include information on the physical properties of the model as phenomenological modeling problems (Figure 1).

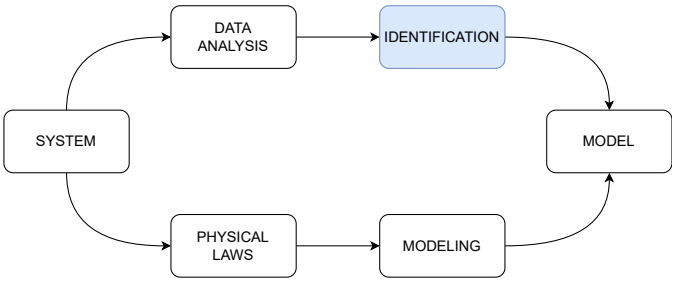

Figure 1. Schematic diagram of the process of obtaining a model that represents a dynamic system.

In the state-space representation, parameters in linear equations interconnect the input and output data (Nise (2020)). The system model can be represented by four principal matrices in the state-space equations as follows:

$$\begin{cases} \dot{\mathbf{X}} = \mathbf{AX} + \mathbf{BU} \\ \mathbf{Y} = \mathbf{CX} + \mathbf{DU} \end{cases} \tag{1}$$

These matrices can be derived using specialized algorithms tailored for this purpose, such as N4SID (*Numerical Algorithms for Subspace State Space System Identification*) and MOESP (*Multivariable Output-Error State Space*).

2.2 Least Squares

The dynamics of a system can be encapsulated in a linear equation relating input and output at a specific discrete time, incorporating an error term $\boldsymbol{\varepsilon}$, as represented in the following equation:

$$\mathbf{Y} = \mathbf{\Phi\Theta} + \boldsymbol{\varepsilon} \tag{2}$$

The problem can be articulated by omitting error values, such as determining the parameter matrix $\mathbf{\Theta}$, based on a matrix of input and output samples, $\mathbf{\Phi}$. The solution that minimizes the error between the actual and predicted values, as developed in Gauss and Stewart (1995), is encapsulated in the following equation:

$$\hat{\mathbf{\Theta}} = [\mathbf{\Phi}^T\mathbf{\Phi}]^{-1}\mathbf{\Phi}^T\mathbf{Y} \tag{3}$$

The least squares estimator is pivotal within the MOESP algorithm, but its utility extends beyond this application. It is a fundamental tool for solving various linear problems in mathematics, science, and engineering disciplines. Due to its versatility and effectiveness, the least squares method is indispensable in numerous scenarios.

2.3 Hankel Block Matrix

A Hankel matrix $\mathbf{H}$ is a special matrix characterized by having constant elements $\mathbf{H}_{ij}$ along its skew diagonals, such that $\mathbf{H}_{ij} = \mathbf{H}_{(i+1),(j-1)}$. An example of a $\mathbf{H}_{m\times n}$ matrix can be given as follows:

$$\mathbf{H} = \begin{bmatrix} h_1 & h_2 & h_3 & \dots & h_n \\ h_2 & h_3 & h_4 & \dots & h_{n+1} \\ h_3 & h_4 & h_5 & \dots & h_{n+2} \\ \vdots & \vdots & \vdots & \ddots & \vdots \\ h_m & h_{m+1} & h_{m+2} & \dots & h_{m+n-1} \end{bmatrix} \tag{4}$$

In subspace identification algorithms, the data is represented in blocks of Hankel matrices, where it is possible to separate input and output samples from a system of order n into blocks of the same dimension, as stated by Overschee and Moor (1995). To construct it, given N samples, the order of the Hankel matrix is established so that the relationship described in the Equation (5) is maintained and $k \geq n$ and $j \gg k$, resulting in a matrix of dimension $i \times j$, considering $k, i, j, n, N \in \mathbb{N}$.

$$j = N - k + 1 \tag{5}$$

The Block Hankel matrix $\mathcal{H}$ used in identification algorithms for a system with n_e inputs and n_s outputs is thus composed by stacking two blocks of Hankel matrices: one for the input samples $\mathcal{U}_{k\cdot n_e \times j}$ and another for the output samples $\mathcal{Y}_{k\cdot n_s \times j}$. This definition can be observed in the Equation (6):

$$\mathcal{H} = \begin{bmatrix} \mathcal{U} \\ \mathcal{Y} \end{bmatrix} = \left[\begin{array}{ccccc} u_0 & u_1 & u_2 & \dots & u_{j-1} \\ u_1 & u_2 & u_3 & \dots & u_j \\ \vdots & \vdots & \vdots & \ddots & \vdots \\ u_i & u_{i+1} & u_{i+2} & \dots & u_{i+j-1} \\ \hline y_0 & y_1 & y_2 & \dots & y_{j-1} \\ y_1 & y_2 & y_3 & \dots & y_j \\ \vdots & \vdots & \vdots & \ddots & \vdots \\ y_i & y_{i+1} & y_{i+2} & \dots & y_{i+j-1} \end{array}\right] \tag{6}$$

where $i = k(n_e + n_s)$ and $j = N - k + 1$.

3. MOESP: MULTIVARIABLE OUTPUT-ERROR STATE SPACE

The MOESP (Multivariable Output-Error State Space) algorithm is used in system identification to estimate the state-space models of dynamic systems. This algorithm comes in two main variants: deterministic and stochastic. The deterministic variant assumes a noise-free environment, focusing solely on deterministic inputs to identify the system's parameters without accounting for disturbances or noise. On the other hand, the stochastic variant includes two primary approaches: MOESP-PI (Past Input) and MOESP-PO (Past Output). MOESP-PI emphasizes the influence of past inputs on the current state and outputs, while MOESP-PO focuses on the relationship between past outputs and the current state. These stochastic methods incorporate noise into the model, making them more robust for real-world applications. Both variants rely on matrix decompositions to derive the state-space representation from input-output data.

Only the deterministic MOESP method will be considered, as the focus is on analyzing its functioning, including its advantages and disadvantages. By concentrating on the

noise-free scenario, we aim to explore the method's effectiveness in ideal conditions, which will provide a clearer understanding of its core capabilities and limitations.

3.1 Matrix Decompositions

The QR decomposition is a matrix decomposition where a matrix with linearly independent columns $\mathbf{A}_{m\times n}$ represents the multiplication of an orthonormal matrix $\mathbf{Q}$ with an upper triangular matrix $\mathbf{R}$ as follow:

$$\mathbf{A} = \mathbf{QR} = [Q_1 \ Q_2] \begin{bmatrix} 0 & R_{12} \\ R_{21} & R_{22} \end{bmatrix} \tag{7}$$

Another option for decomposing matrices is through Singular Value Decomposition (SVD), in which any matrix $\mathbf{A} \in \mathbb{R}^{m\times n}$ can be represented through two orthogonal matrices $\mathbf{U} \in \mathbb{R}^{m\times m}$ and $\mathbf{V} \in \mathbb{R}^{n\times n}$ and a diagonal matrix $\mathbf{\Sigma} \in \mathbb{R}^{m\times n}$ as follows:

$$\mathbf{A} = \mathbf{U\Sigma}V^T \tag{8}$$

Singular Value Decomposition (SVD) is a technique in multiple disciplines, notably signal processing and data analysis. In dynamic systems identification, SVD is frequently employed to condense data dimensionality, elucidate significant patterns, and filter out noise. This application improves the accuracy and efficiency of the resulting models.

3.2 MOESP Algorithm Implementation

This section presents the implementation of the MOESP algorithm, detailing each workflow step. The process is illustrated in Figure 2, which visually represents the algorithm's sequence and operations, enhancing the understanding of its practical application.

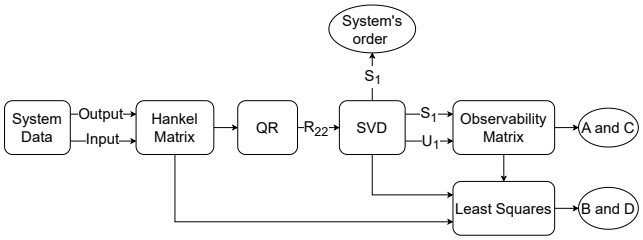

Figure 2. MOESP Algorithm Workflow.

The first step in implementing the MOESP algorithm is constructing the Hankel matrix. This matrix is built by organizing the input and output data into a structured form, with each block representing a segment of the system's response over time. The order of the Hankel matrix k must be chosen in this step as it influences the effectiveness of the algorithm in capturing the system's dynamics.

The second step involves the QR decomposition of the Hankel matrix, which transforms it into two matrices: an orthonormal matrix $\mathbf{Q}$ and an upper triangular matrix $\mathbf{R}$. Specifically, the matrix R_{22}, derived from this decomposition as detailed in Equation 7, represents the lower triangular part of $\mathbf{R}$ and will be used in the subsequent steps of the algorithm. Geometrically, this decomposition projects the input data onto the output data.

The next step involves performing Singular Value Decomposition (SVD) on the matrix R_{22}, which results in three matrices: $\mathbf{U}_1$, $\mathbf{S}_1$, and $\mathbf{V}_1$. For the algorithm, only $\mathbf{U}_1$ and $\mathbf{S}_1$ will be used. In the context of the studied algorithm, this decomposition allows the extraction of the main characteristics of the matrix that projects the output data onto the input data, reducing its dimensionality.

In situations where system information is not available, the method developed in Overschee and Moor (1995) provides a way to estimate the system order $\hat{\mathbf{n}}$ by analyzing the singular values in the matrix $\mathbf{S}_1$. Since these singular values are arranged in descending order, the system order can be estimated by identifying the index of the singular value where the cumulative sum of the absolute values exceeds 90% of the total.

The resulting matrices from these transformations, as shown also in the work of De Moor et al. (1997), can be related to the extended observability matrix to find the matrices $\mathbf{A}$ and $\mathbf{C}$. At the same time, the matrices $\mathbf{B}$ and $\mathbf{D}$ are determined through algebraic manipulations.

In Equation (9), the relationship between the extended observability matrix $\mathbf{\Gamma}$, the matrix $\mathbf{A}$, and the matrix $\mathbf{C}$ is demonstrated. At this stage in the algorithm, defining the system order n becomes crucial, as it directly impacts the construction and analysis of the observability matrix.

$$\mathbf{\Gamma} = \begin{bmatrix} \mathbf{C} \\ \mathbf{CA} \\ \mathbf{CA}^2 \\ \vdots \\ \mathbf{CA}^{n-1} \end{bmatrix} = \mathbf{U}_1\mathbf{S}_1^{1/2} \tag{9}$$

In Equation (10), demonstrated in De Moor et al. (1997), the extended observability matrices $\mathbf{\Gamma}$, composed of input and output samples, are related to the Toeplitz matrix T, which connects the state-space equation matrices.

$$\mathbf{\Gamma}_i^{\perp}\mathbf{Y}_f\mathbf{U}_f^{\dagger} = \mathbf{\Gamma}_i^{\perp}T_i \tag{10}$$

4. EXPERIMENTAL RESULTS

This section presents the results of applying the MOESP identification method to a real coupled tank system. The algorithm calculates the matrices that define the systems' dynamics from the data collected based on different free variables (estimated system order). We used a simulated and a real system to validate the methodology.

4.1 Simulated System

The first system to be analyzed is a numerical and simulated dynamic system characterized by three discrete random inputs and four random matrices $\mathbf{A}_s$, $\mathbf{B}_s$, $\mathbf{C}_s$, and $\mathbf{D}_s$, which define its behavior and result in two outputs. We generated all variables using the *NumPy* library in the *Python* language, producing 2,000 input data points (Figure 3) and 2,000 noisy output data points (Figure 4), which will be provided to the MOESP algorithm. The matrices used for this analysis are described below:

$$\mathbf{A}_s = \begin{bmatrix} 0.603 & 0.603 & 0 & 0 \\ -0.603 & 0.603 & 0 & 0 \\ 0 & 0 & -0.603 & -0.603 \\ 0 & 0 & 0.603 & -0.603 \end{bmatrix}$$

$$\mathbf{B}_s = \begin{bmatrix} 1.1650 & -0.6965 \\ 0.6268 & 1.6961 \\ 0.0751 & 0.0591 \\ 0.3516 & 1.7971 \end{bmatrix}$$

$$\mathbf{C}_s = \begin{bmatrix} 0.2641 & -1.4462 & 1.2460 & 0.5774 \\ 0.8717 & -0.7012 & -0.6390 & -0.3600 \end{bmatrix}$$

$$\mathbf{D}_s = \begin{bmatrix} -0.1356 & -1.2704 \\ -1.3493 & 0.9846 \end{bmatrix}$$

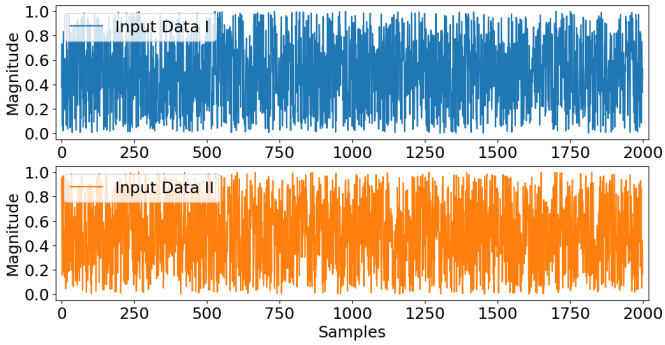

Figure 3. Simulated System Input Values.

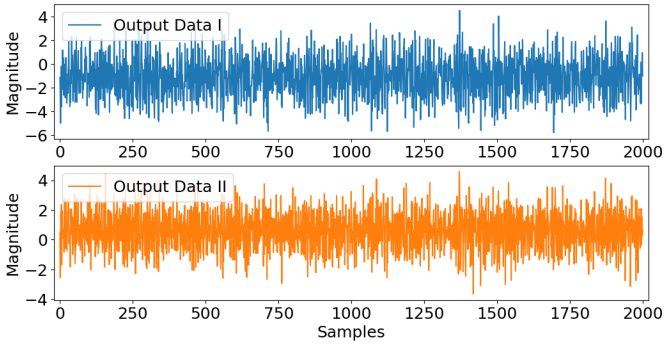

Figure 4. Simulated System Output Values.

Given the familiarity with this specific system, the algorithm will be applied to the presented data and analyzed using another set of 2,000 input samples and 2,000 output samples generated by the same state-space equations of this fourth-order system.

To explore the choices of the algorithm's free variables, we compared the results across three different system orders, including the order estimated by the algorithm using the singular values of matrix $\mathbf{S}_1$. The magnitude of the singular values for the simulated system is analyzed in Figure 5. The order $\hat{n} = 4$ encompasses 90% of the system's information, making it the primary order. The remaining orders ($\hat{n}_2 = 3$ and $\hat{n}_3 = 5$) are also investigated.

The figure below graphically compares the results obtained from the MOESP algorithm with different system orders for both outputs of the Simulated System.

The table below evaluates the samples estimated by the MOESP algorithm for the Simulated System, considering the different system orders studied. The values of Mean Absolute Error (MAE), Mean Squared Error (MSE), Root

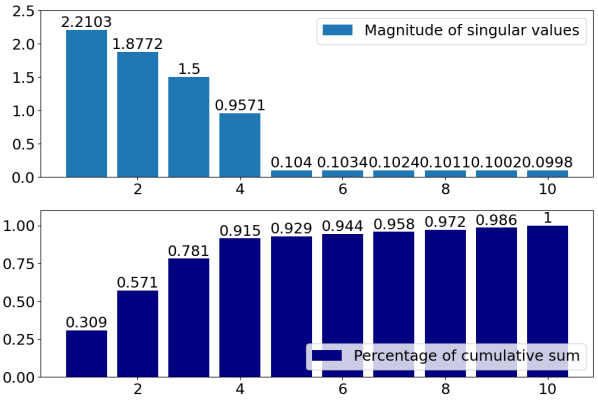

Figure 5. Singular values obtained from matrix $\mathbf{S}_1$ (above subplot) and the percentage of the cumulative sum of these values (below subplot) for the Simulated System.

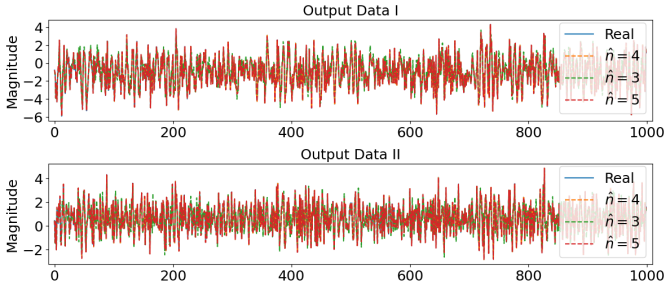

Figure 6. Comparison of MOESP Algorithm Results for Different System Orders in the Simulated System.

Mean Squared Error (RMSE), Coefficient of Determination (R^2), and Variance Accounted For (VAF) are reported for each output and system order.

Table 1. Evaluation of the samples estimated by the MOESP algorithm with different orders compared to the reference samples for the Simulated System.

Output	Order	MAE	MSE	RMSE	R^2	VAF
I	$\hat{n}_1 = 4$	0.01	0	0.01	1	100
	$\hat{n}_2 = 3$	0.57	0.51	0.71	0.83	84.09
	$\hat{n}_3 = 5$	0.01	0	0.01	1	100
II	$\hat{n}_1 = 4$	0.01	0	0.01	1	100
	$\hat{n}_2 = 3$	0.37	0.22	0.47	0.86	85.94
	$\hat{n}_3 = 5$	0.01	0	0.02	1	100

Based on the results presented in the table, it is evident that the performance of the MOESP algorithm in estimating samples for the Simulated System varies according to the considered system order for both outputs. The estimates show excellent performance for each output when the system order is $\hat{n}_1 = 4$ and $\hat{n}_3 = 5$, indicating almost exact agreement with the reference values. However, for the order $\hat{n}_2 = 3$, although there is still a good performance, the values found in the evaluation metrics suggest slightly lower adequacy than the other models for both outputs.

Additionally, we noted that when the estimated system order coincides with that of the reference system ($\hat{n}_1 = 4$), the matrices describing the simulation system's dynamics differ. This variation reflects a fundamental characteristic

of the matrix representation of systems: its ability to represent a system in multiple ways. Thus, a subspace that captures its main characteristics can describe and identify any system in a matrix space.

4.2 Coupled Tank System

The second system used to validate the MOESP algorithm is the Coupled Tanks System Ícaro Araújo et al. (2019), as shown in the diagram in Figure 7, where there are four tanks with valves at the bottom through which water flows, supplied by two electric motors. The changes

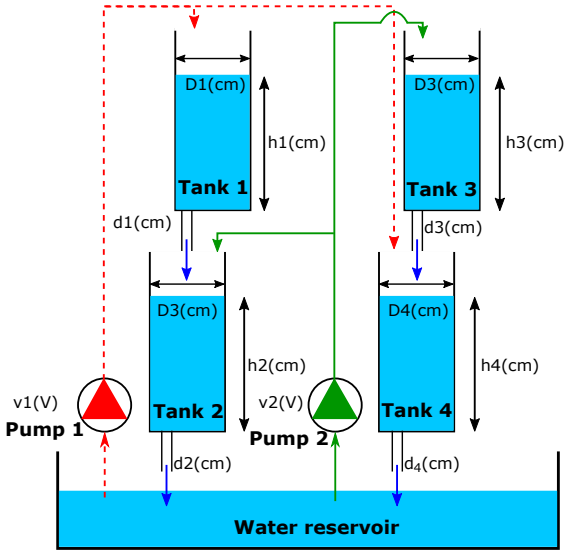

Figure 7. Diagram for the Coupled Tanks (Source: Ícaro Araújo et al. (2019)).

The experiment conducted for data collection lasted for 500 seconds with a sampling time of $t = 0.1$s. The voltages applied to the two motors (Figure 8) attempt to approximate a persistently exciting input to reveal the characteristics of the studied system as much as possible. Similarly, throughout the entire experiment period, the outputs (Figure 9) were also collected at the same sampling time t.

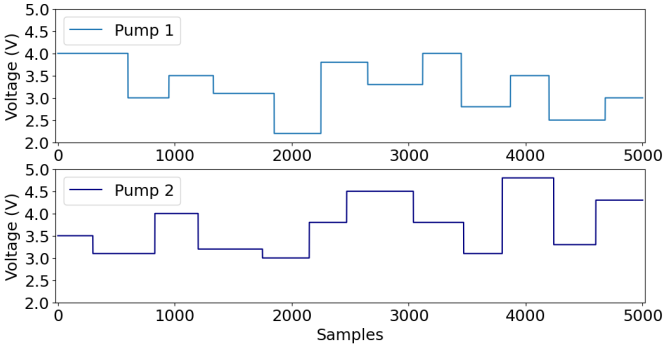

Figure 8. Input values of the experiment with the Coupled Tanks System.

In this experiment, the order of the Hankel matrix will be fixed as $k = 2$, while the estimated orders vary around the standard system order calculated by the singular values. Figure 4.2 graphically shows the singular values of matrix $\mathbf{S}_1$ in descending order, along with the percentage of the cumulative sum.

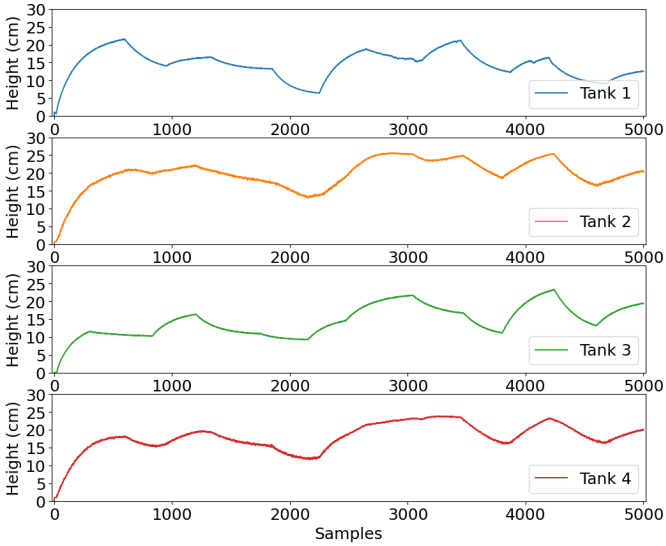

Figure 9. Output values of the experiment with the Coupled Tanks System.

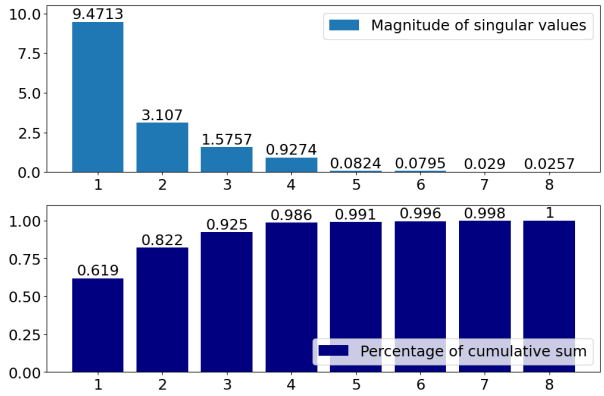

Figure 10. Singular values obtained from matrix $\mathbf{S}_1$ (upper subplot) and the percentage of the cumulative sum of these values (lower subplot) for the Coupled Tanks.

Thus, the first three largest singular values already encompass more than 90% of the total cumulative sum. Therefore, the standard estimated order of the system for constructing matrices of state-space equations will be $\hat{n}_1 = 3$. The other studied orders will be $\hat{n}_2 = 2$ and $\hat{n}_3 = 4$. The figure below graphically compares the results for each order $\hat{n}$ of the Coupled Tanks System.

Using a numerical analysis of the estimation made by MOESP, we considered the following metrics: Mean Absolute Error (MAE), Mean Squared Error (MSE), Root Mean Squared Error (RMSE), Coefficient of Determination (R^2), and Variance Accounted For (VAF). Table 2 presents the metrics separated by output and the estimated order inserted into the algorithm.

The MOESP algorithm's effectiveness in nonlinear system contexts is again highlighted, along with the influence of the estimated order on the results. In the case of the Coupled Tanks, it is evident that the best performance was not achieved by following the standard order calculated by the singular values. This fact suggests that prior knowledge of the system plays a crucial role in the system

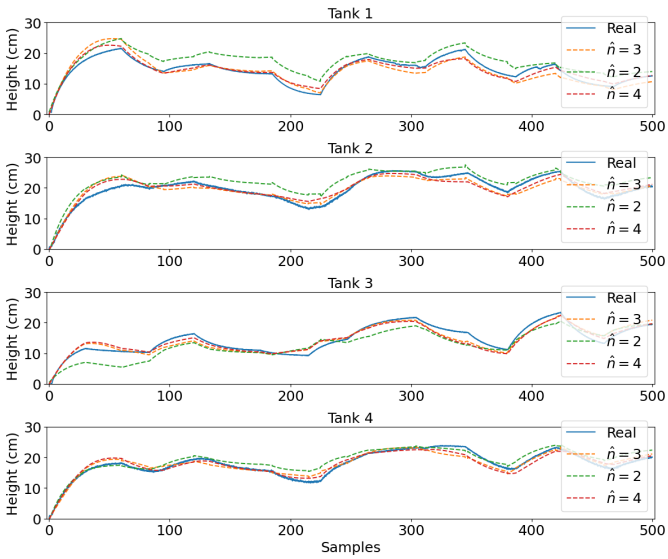

Figure 11. Comparison of MOESP Algorithm Results for Different System Orders in the Coupled Tank System.

Table 2. Evaluation of samples estimated by the MOESP algorithm with different orders compared to reference samples for the Coupled Tanks System.

Tank	Order	MAE	MSE	RMSE	R^2	VAF
1	$\hat{n}_1 = 3$	1.575	3.509	1.873	0.753	76.206
	$\hat{n}_2 = 2$	2.901	10.572	3.251	0.255	84.798
	$\hat{n}_3 = 4$	1.058	1.669	1.292	0.882	88.232
2	$\hat{n}_1 = 3$	1.316	2.587	1.608	0.852	85.44
	$\hat{n}_2 = 2$	2.394	7.446	2.729	0.574	89.953
	$\hat{n}_3 = 4$	1.173	2.019	1.421	0.885	88.477
3	$\hat{n}_1 = 3$	1.259	2.12	1.456	0.885	88.842
	$\hat{n}_2 = 2$	2.247	6.69	2.587	0.637	77.736
	$\hat{n}_3 = 4$	1.187	2.054	1.433	0.888	89.196
4	$\hat{n}_1 = 3$	1.008	1.612	1.269	0.894	89.416
	$\hat{n}_2 = 2$	1.401	3.024	1.739	0.801	89.325
	$\hat{n}_3 = 4$	0.925	1.294	1.138	0.915	91.499

identification, underscoring the importance of considering additional information during modeling and analysis.

Table 3. Evaluation of samples estimated by NARX models. Source: Ícaro Araújo et al. (2019).

Method/Output	Tank 1	Tank 2	Tank 3	Tank 4
FROLS	0.0343	0.0946	0.0425	0.0885
SEMP	0.0342	0.0923	0.0408	0.0867

Comparing the results presented in Ícaro Araújo et al. (2019) with the data in Table 3, it is observed that the performance of the explored NARX models exceeds the best case obtained by subspace methods. However, it is essential to note that this superiority occurs in a low-complexity system context. In more complex systems, NARX models require greater computational capacity and a well-defined structure for process identification. This need to determine the model structure may pose an additional challenge compared to subspace methods, which typically offer a more structured and interpretable approach to modeling.

5. CONCLUSION

This study addressed some of the main works related to the system identification problem and how it can be solved using subspace methods. The main focus was to analyze the MOESP algorithm and its relevance in this context, highlighting the need to explore it from different perspectives. All relevant mathematical concepts were presented and discussed in detail. An essential aspect addressed was the free variable associated with the choice of system order, whose influence on the estimated results was investigated for different system examples.

The development of this work achieved its objective by explaining and exploring the MOESP algorithm in different types of systems and various orders. In doing so, it was possible to observe the significant impact of the choice of free variables on the estimated system response and the feasibility of calculating these variables using the matrices found within MOESP itself, resulting in the best results among those mathematically analyzed.

For future work, we propose that other methods, such as N4SID and CVA, can be explored, like MOESP, involving a detailed analysis of the underlying mathematics of the algorithms, followed by applying these methods to different systems and variations of the free variables. Additionally, the investigation can be expanded beyond the system order, also exploring the influence of the Hankel matrix order on the estimated results. By conducting this comparative analysis, it will be possible to discern which method better suits different scenarios and discuss their advantages and limitations more precisely and groundedly.

REFERENCES

Bauer, D. (2001). Order estimation for subspace methods. *Automatica*, 37, 1561–1573. doi:10.1016/S0005-1098(01)00118-2.

De Moor, B., De Gersem, P., De Schutter, B., and Favoreel, W. (1997). DAISY: A database for identification of systems. *Journal A*, 38(3), 4–5.

Gauss, C.F. and Stewart, G.W. (1995). *Theory of the Combination of Observations Least Subject to Errors, Part One, Part Two, Supplement*. Society for Industrial and Applied Mathematics. doi:10.1137/1.9781611971248.

Nise, N.S. (2020). *Control systems engineering*. John Wiley & Sons.

Overschee, P.V. and Moor, B.D. (1995). Choice of state-space basis in combined deterministic-stochastic subspace identification. *Autom.*, 31(12), 1877–1883. doi:10.1016/0005-1098(95)00071-9.

Zhou, K., Wang, Z., Gao, Q., Yuan, S., and Tang, J. (2023). Recent advances in uncertainty quantification in structural response characterization and system identification. *Probabilistic Engineering Mechanics*, 74, 103507. doi:https://doi.org/10.1016/j.probengmech.2023.103507. URL `https://www.sciencedirect.com/science/article/pii/S0266892023000966`.

Ícaro Araújo, Cavalcante, G., Lúcio, Y., and Araújo, F. (2019). Nonlinear system identification of a mimo quadruple tanks system using narx model. *Przegląd Elektrotechniczny*, 95(6), 66–72. doi:10.15199/48.2019.06.12.